

Prediction of Thread Milling Instantaneous Cutting Forces

B. Moetakef Imani*, **H. Abdollahzadeh***, **H. El-Mounayri****

**Mechanical Engineering Department, Engineering Faculty
Ferdowsi University of Mashhad, Mashhad, Iran*

*** Department of Mechanical Engineering, IUPUI, Indianapolis, USA
imani@um.ac.ir*

Abstract: This research presents a new model for the prediction of thread milling forces. Cutting constants for AL 7075-T6 are calculated by the well-known orthogonal to oblique method. First, the thread milling cutting mechanism is described and then mechanics of cutting for thread milling is analyzed similar to that of the end milling process. The instantaneous chip load is computed based on the modified cutting edge geometry for an ISO standard threads mill. To achieve experimental forces, 'KISTLER 9255 B' dynamometer is incorporated in the setup. Finally, experimental and simulated forces are compared. The results indicate that the proposed model could predict cutting forces of thread milling accurately.

Key words: Thread milling, orthogonal to oblique cutting, force model

1. INTRODUCTION

Threads on a work-piece can be manufactured in variety of ways using the two fundamental approaches: plastic deformation and metal cutting. Threads produced by plastic deformation are normally stronger but thread forming processes can not achieve the high accuracy which is required in many applications. Also, threads made in brittle materials such as cast iron cannot be produced by plastic working. The alternative approach for thread generation is thread cutting. The common cutting processes are tapping, die threading, and turning [Stephenson *et al.*, 1996]. These processes are very limited due to the fact that in tapping and die threading, the tool nominal diameter should be the same as the hole diameter [DeGarmo *et al.*, 1999]. Also tapping and die threading tools are right or left handed and using a same tool for both operations is impossible. The thread milling method is introduced in industry for generating accurate left or right handed threads which also can be used for internal and external threads. In thread milling operations, the tool diameter does not depend to the hole or shaft diameter. In addition, dimensional and angular accuracy of thread milling is much better than former processes [Koelsch *et al.*, 1995, Halas *et al.* 1996]. Furthermore, thread milling provides better chip evacuation than tapping, leading to less tool wearing or tool breakage due to chip clogging and increased friction. Thread cutting on conical surface is another advantage of thread milling.

A number of force models have been developed for predicting cutting forces in tapping and serrated-end milling, which seems have a similar geometric features with the thread mill [Dogra *et al*, 2002, Armarego *et al* 2002, Campomanes *et al*, 2002, Merdol *et al* 2004]. However, these force models cannot be used for thread milling due to different cutting movements and cutting edge profiles. There are very limited researches on the cutting characteristics of the thread milling process. A. C. Arjoo has presented a model for prediction of thread milling forces. In the developed model, the chip thickness is calculated to incorporate varying radial depth of cut along the cutting edge. Also, the influence of tool run out is considered. A cutting force model is proposed by using the mechanistic approach [A.C. Araujo *et al.*, 2005]. The main objective of this paper is to develop a thread milling force model that can be used to understand the thread milling process and consequently to enhance the process performance. The instantaneous chip thickness model is developed to incorporate varying radial depth of cut along the cutting edge. The tool is modeled as an end mill with thread edge profile according to ISO standard threads. The proposed thread milling force model is verified by a variety of experiments.

Henceforth, this paper is organized as follows. The characteristics of the thread milling process are described in Section 2. The tool geometry of a thread mill is modeled and the chip thickness and cutting force model development are presented in the following section. The chip load modeled in MATLAB and compared with the results of computation in ACIS software which is presented in Section 4. The cutting constants are then calculated using the orthogonal to oblique approach. To verify the proposed force model, a series of experiments were conducted on SMTCL (VMC-850) CNC Milling center and thread milling forces are measured using a KISTLER three-axis dynamometer. Lastly simulated and experimental forces compared the results shows that this model could accurately predict cutting force in thread milling.

2. TOOL MOVEMENT

The machining process of thread milling can be implemented in five stages as shown in figure 1. The first stage involves positioning the tool with the center axis of the hole and then lowering the tool into position to begin thread milling. When the tool positioned with the prescribed rotational speed, it moves toward the work piece at the desired feed rate and reach the required radial depth of cut. In the third stage, the tool moves helically at a given feed rate for one complete revolution. The number of threads generated in this one revolution corresponds to the number of threads engaged in the work piece. If generation of the threads for the full depth of the hole is achieved in several steps, the stages 1–3 are repeated until all the threads are generated. Once the threads are generated, the tool moves back to the center of the hole (fourth stage). Finally, the tool is retracted out of the hole [A.C. Araujo *et al.*, 2005].

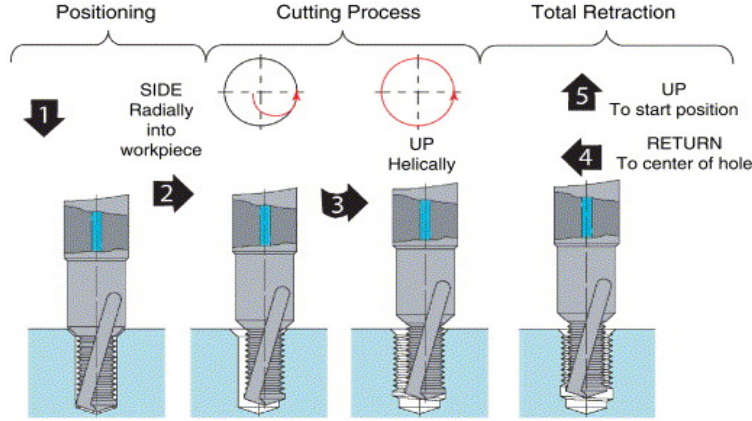


Figure 1; machining process of thread milling [A.C. Araujo et al., 2005]

3. TOOL GEOMETRY MODELING

The tool geometry is presented in figure 2, where the helix angle λ is defined. The outside and inside diameters of the tool are denoted as d_e and d_i , respectively. The thread is characterized by the thread angle ξ , thread pitch p , and thread height H . In cylindrical coordinate system, each point on cutting edge p is shown by a vector \mathcal{R} from origin to the point, see figure 3.

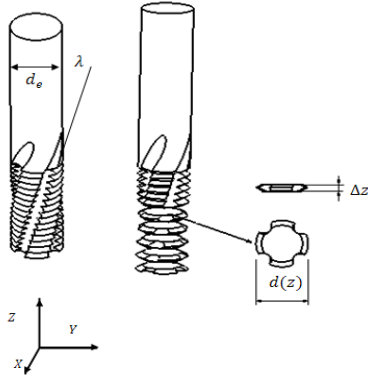


Figure 2; tool geometry

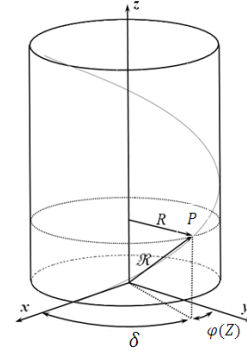


Figure 3; cylindrical coordinate system

$$\mathbf{R} = R_x \vec{i} + R_y \vec{j} + R_z \vec{k}$$

$$R_x = R \times \sin \varphi(z)$$

$$R_y = R \times \cos \varphi(z)$$

$$R_z = z$$

$$\varphi(z) = \frac{\tan(\lambda)}{\left(\frac{dE}{2}\right)} \times Z$$

(1)

(2)

Where R is radial distance between point p and Z axis. In end milling, there is no variation in tool diameter and R described as tool radius. But in thread milling, the diameter varies along the tool axis. In equations 1, $\varphi(z)$ is the angle of between Y axis and the projection of point p on x - y plane calculated by equation 2. The variation of tool diameter for a thread

mill is related to the pitch and the thread profile which can be obtained by equation 3. The thread milling tool can be analyzed as a stack of disks, 1, N_z where each disk has Δz thickness and a variable diameter $d(Z)$ as shown in figure 2 [A.C. Araujo *et al.*, 2005].

$$d(Z) = \begin{cases} di + \frac{2(Z - nt(Z) p/2)}{\tan(\xi)} & \text{if } nt(Z) \text{ is odd} \\ de - \frac{2(Z - nt(Z) p/2)}{\tan(\xi)} & \text{if } nt(Z) \text{ is even} \end{cases} \quad (3)$$

$$nt(z) = \text{Integer part} \left[\frac{2z}{p} \right] \quad (4)$$

The variation in the disk diameter along the tool axis causes different radial depth of cut for each disk which will be described later on. The angle between the flutes depends on the numbers of flutes Nf and is defined by equation 5.

$$\theta_p = \frac{2\pi}{Nf} \quad (5)$$

The modeled tool geometry for a four flutes tool with helix angle 15° , tool height 30mm and pitch 1.5 mm is shown in figure 4. The nominal thread height is calculated by equation 6 but according to ISO metric standard threads commonly used in industry.

$$H = \cos 30 \times p = 0.866 \times p \quad (6)$$

In figure 5 specifications of nuts and bolts in ISO standard are shown. Where p is the thread pitch and d, d_1, D, D_1 are in order bolt external diameter, bolt internal diameter, nut external diameter and Nut internal diameter. This paper is considered a ISO standard thread thus specifications are described. ISO standard is based on SI system and some major specifications are as follows. The thread angle is 60° , the tip of bolt's thread is chamfered by $\frac{H}{8}$, bolt's thread bottom is filleted by radius of $\frac{H}{6}$, the tip of nut's thread is chamfered by $\frac{H}{4}$ and nut's thread bottom is also chamfered by $\frac{H}{8}$, refer to figure 6 for details.

It is obvious that bolt's and nut's thread height are not equal in ISO standard and expressed by equation 7 and equation 8, respectively.

$$h = H - \left(\frac{H}{8} + \frac{H}{6} \right) = 0.6134 \times p \quad (7)$$

$$t = H - \left(\frac{H}{8} + \frac{H}{4} \right) = 0.5413 \times p \quad (8)$$

In the work ISO standard nut thread is considered and modeled, see figure 7. It is clear that the thread milling cutting forces should be based the above mentioned tool geometry.

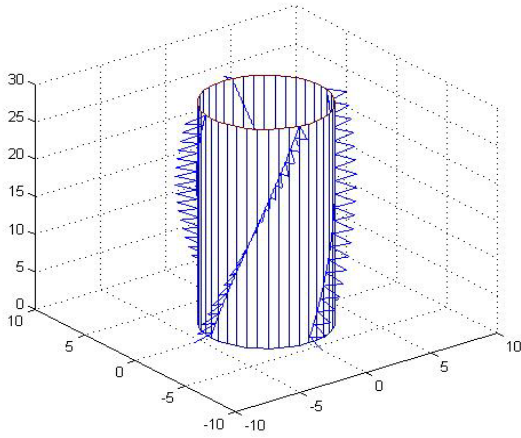


Figure 4; Tool modeled geometry

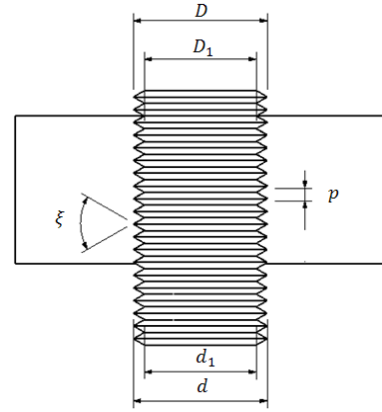


Figure 5 ; Nut and bolt

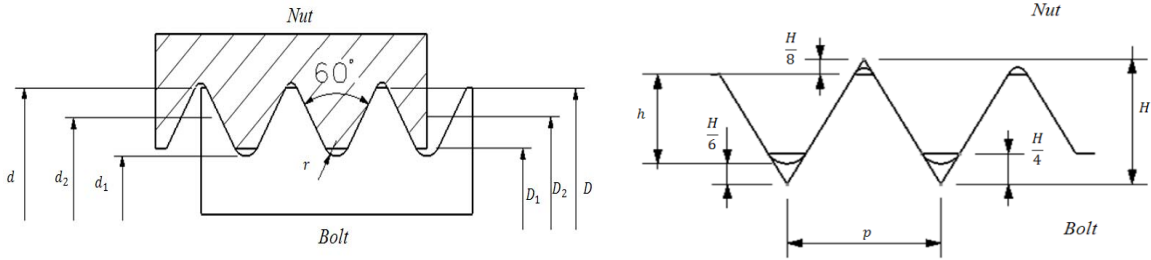


Figure 6; Nut and bolt dimensions in ISO standard

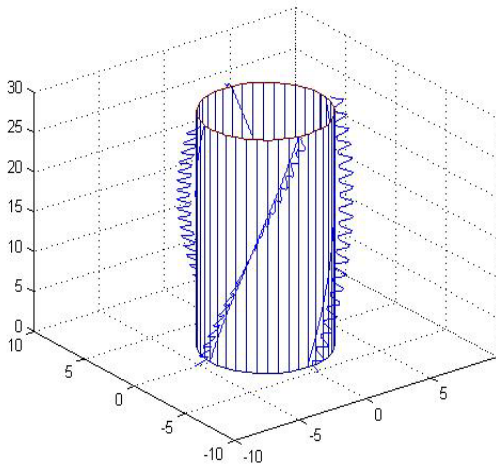


Figure 7; ISO modeled thread mill

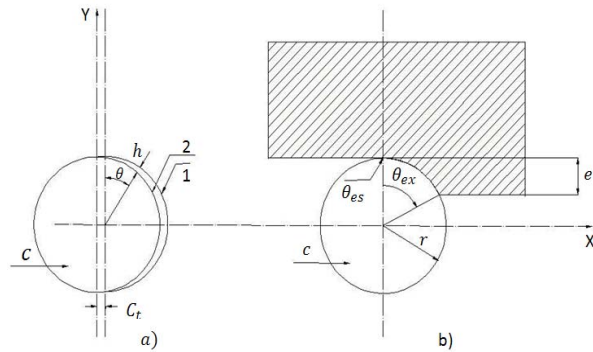


Figure 8; cutting zone

4. CHIP LOAD AND CUTTING FORCE MODELING

As previously expressed, the thread mill can be analyzed as a stack of disks where each disk has Δz thickness and variable diameter $d(Z)$. The disk number, the flute number and

rotation angle are in order denoted by (N, i, θ) . The cutting exit angle for each disk should be calculated according to its disk diameter $d(Z)$. Thus, in contrast to end milling, the exit angle is not constant along the cutting edge. The cutting force acting on each disk can be decomposed to tangential, radial and axial directions, and expressed by equation 9. In each tool rotation increment, the number of cutting edge engaged should be firstly determined. Then, the cutting force components on each cutting edge should be calculated. Total cutting force will be determined by iteration of above mentioned algorithm.

$$\begin{aligned}\Delta F_t(N, i, \theta) &= K_{tc}\Delta bh + K_{te}\Delta b \\ \Delta F_r(N, i, \theta) &= K_{rc}\Delta bh + K_{re}\Delta b \\ \Delta F_a(N, i, \theta) &= K_{ac}\Delta bh + K_{ae}\Delta b\end{aligned}\quad (9)$$

Where ΔF_t , ΔF_r and ΔF_a are tangential, radial and axial differential forces on each disk. Also, Δb is axial depth of cut (or Δz), h is chip load and will be determined by equation 10. According figure 8-a h is radial difference between path 1 and 2. In equation 9 the cutting constants in tangential, radial and axial directions are denoted by (K_{tc}, K_{rc}, K_{ac}) . Also, the cutting edge constants in tangential, radial and axial directions are expressed by (K_{te}, K_{re}, K_{ae}) .

$$h(N, i, \theta) = c_t \sin \theta \quad (10)$$

c_t in equation 10 is feed per tooth. The cutting exit angle θ_{ex} could be determined in each disk by equation 11, see also figure 8-b.

$$\theta_{ex}(N) = \cos^{-1} \left(1 - \frac{2e(N)}{d(N)} \right) \quad (11)$$

Where $e(N)$ called radial depth of cut in each disk which introduced in figure 9 and could be determined by equation 12.

$$e(N) = \frac{d(N) - d_i}{2} \quad (12)$$

Instantaneous elemental cutting forces in tangential, radial and axial directions could be determined by

$$\begin{aligned}dF_t(N, i, \theta) &= K_{tc} c_t \sin \theta \Delta z + K_{te}\Delta z \\ dF_r(N, i, \theta) &= K_{rc} c_t \sin \theta \Delta z + K_{re}\Delta z \\ dF_a(N, i, \theta) &= K_{ac} c_t \sin \theta \Delta z + K_{ae}\Delta z\end{aligned}\quad (13)$$

According to figure 10 force vectors in tangential, radial and axial directions can be projected to (X, Y, Z) directions and computed by

$$\begin{aligned}dF_x(N, i, \theta) &= dF_t(N, i, \theta) \sin \theta - dF_r(N, i, \theta) \cos \theta \\ dF_y(N, i, \theta) &= -dF_t(N, i, \theta) \cos \theta - dF_r(N, i, \theta) \sin \theta \\ dF_z(N, i, \theta) &= dF_a(N, i, \theta)\end{aligned}\quad (14)$$

Finally the resultant cutting force acting on a disk can be achieved by equation 15.

$$dF(N, i, \theta) = \sqrt{dF(N, i, \theta)_x^2 + dF(N, i, \theta)_y^2 + dF(N, i, \theta)_z^2} \quad (15)$$

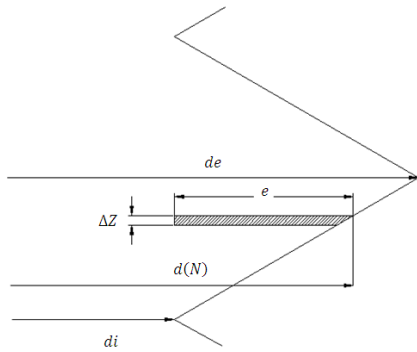


Figure 9; Radial depth of cut in each disk

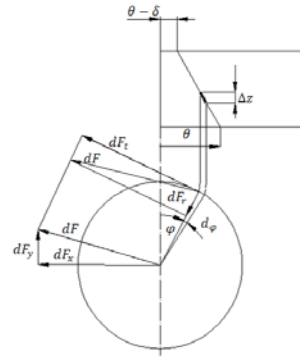


Figure 10; projected forces

The Validity of chip load calculation routine which is written in MATLAB is verified using ACIS software, see figure 11 and 12. For the same cutting conditions, computed chip loads are in precise agreement.

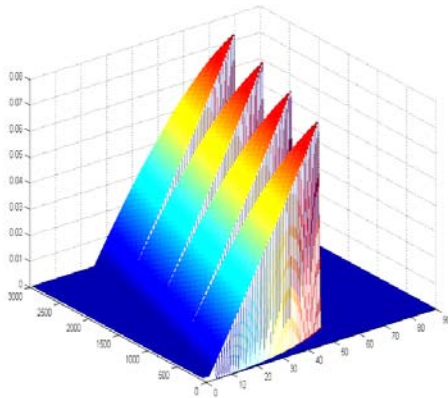


Figure 11; Modeled chip load with MATLAB

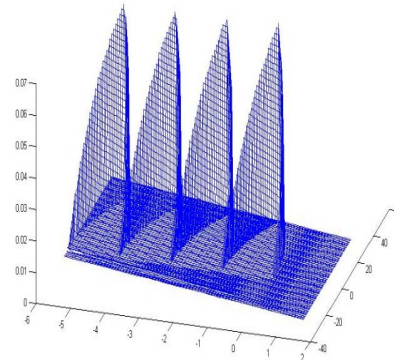


Figure 12 ; Modeled chip load with ACIS

5. CUTTING CONSTANTS

The orthogonal to oblique transform approach [Budak *et al.*, 1996] is used for determining cutting constants. The work piece material is 7075-T6 Aluminum. In order to obtain cutting constants a full factorial matrix for design of experiments is used. The variables are spindle speed, feed, rake angle and depth of cut. The values of spindle speed and feed are (125, 500, 710, 1000) rpm and (0.05, 0.11, 0.22, 0.28) mm per revolution, respectively. Also, the rake angles are selected as (0, 5, 10, 15) degree. In order to create proper conditions of orthogonal cutting tests, aluminum tubes with outside diameter 60mm and thicknesses of (2, 4, 6, 8) millimeter are used. The results are reported in table 1.

Table1- Cutting constants

K_{tc}	K_{rc}	K_{ac}	K_{te}	K_{re}	K_{ae}
820	450	130	20	18	5

6. EXPERIMENTS AND RESULT

In thread milling tests, a standard helical thread milling tool, M12 _ 1:5 ISO used, see figure 13. A series of experiments were conducted on SMTCL (VMC-850) CNC Milling center. A KISTLER three-axis dynamometer (KISTLER 9255 B) was used to acquire three components of the cutting force. A representative view of the experimental setup is shown in figure 14. Since the value of the helix angle is not readily available from the manufacturer, the helix angle λ has been measured by measuring the gap angle Θ as shown in figure 15[A.C. Araujo *et al.*, 2005]. The picture is taken by A 14 megapixel monochrome CCD Flea2 camera made by Point Grey Corp. Once the angle Θ is determined, figure 16, the helix angle can be obtained by equation 16.

$$\lambda = \tan^{-1} \left(\frac{d_i \times \Theta}{p} \right) \quad (16)$$

Where d_i the internal diameter of the thread milling cutter and p is the pitch between the threads. The helix angle for the helical tool was found to be 20° . The cutting conditions used in experiments are $b=6\text{mm}$, spindle speed was 1500 RPM.



Figure 13; used thread mill

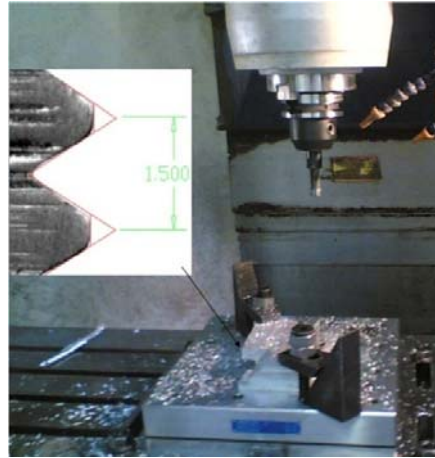


Figure 14; experimental setup

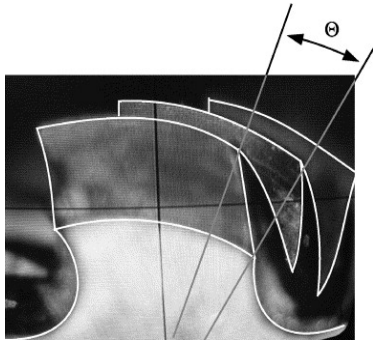
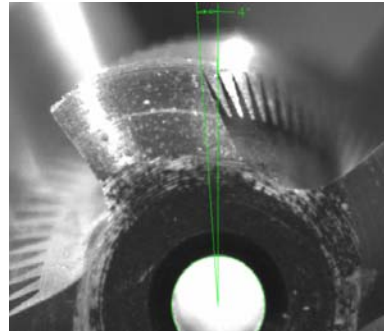


Figure 15; gap angle Θ Figure



16; gap angle Θ on used thread mill

7. RESULTS AND DISCUSSIONS

Figures 17 to 20 show the experimental force measurement results for thread milling on side wall of a block. In this research due to small variations related to the pitch, the z movement is ignored. The simulated x and y components of the cutting force for the given conditions are in a great agreement with the measured forces. It can be noted that the cutting time span of measured and simulated forces are matching and the maximum difference of peak values are within 8.5%.

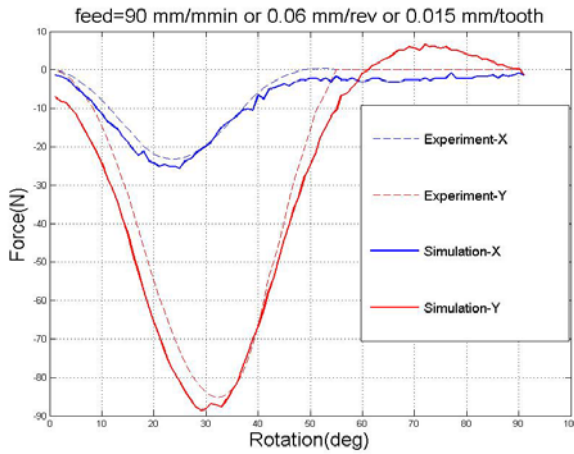


Figure 17; Cutting forces at the feed rate of 90 mm/min

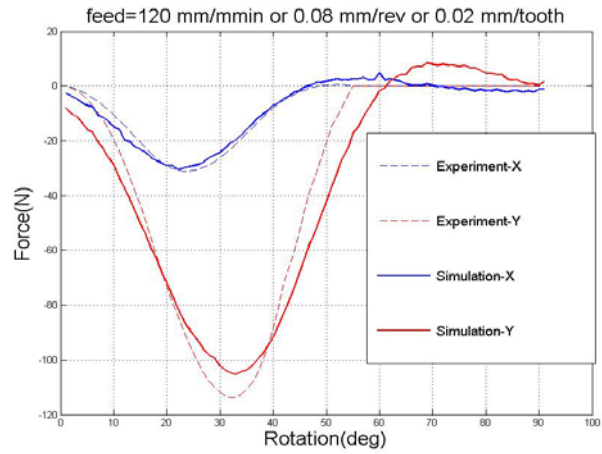


Figure 18; Cutting forces at the feed rate of 120 mm/min

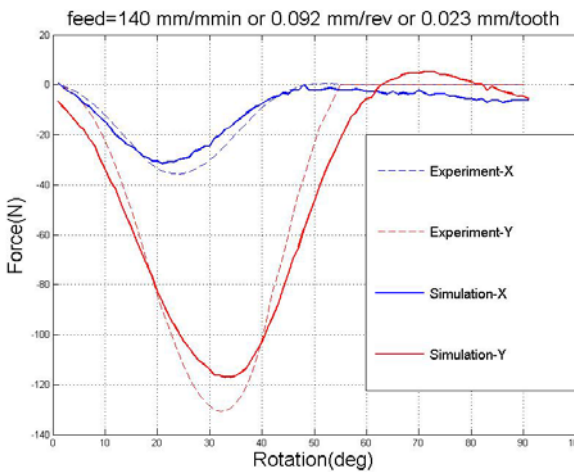


Figure 19; Cutting forces at the feed rate of 140 mm/min

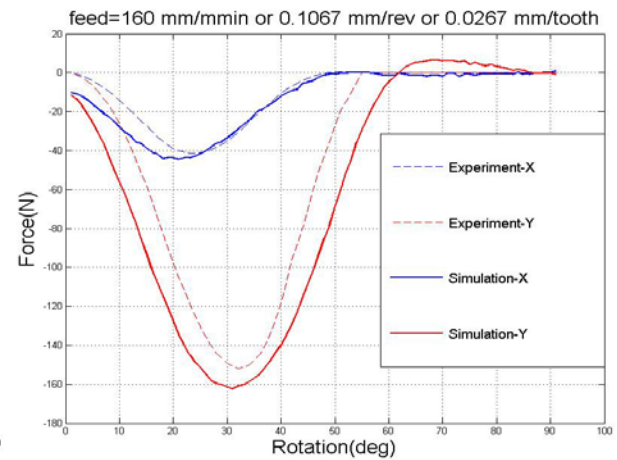


Figure 20; Cutting forces at the feed rate of 160 mm/min

8. CONCLUSION

A model for prediction of thread milling forces is presented in this research. At the first step, AL 7075-T6 cutting constants are calculated. The mechanics of cutting for thread milling is analyzed similar to that of end milling process but cutting edge geometry is modeled according to the ISO standard for threads mill. In order to verify the proposed model an experimental setup is designed which includes forces, KISTLER 9255 B dynamometer. Finally, The results indicate that the proposed model could predict cutting forces of thread milling accurately, thus can be used for various thread milling applications such as thread cutting on thin walled tubes, conical surfaces.

9. REFERENCES

- [Stephenson *et al.*, 1996] D.A. Stephenson, J.S. Agapiou , Metal Cutting Theory and Practice ,Marcel Dekker , New York, 1996.
- [DeGarmo *et al.*, 1999] E.P. DeGarmo , J.T. Black, R.A. Kohser, Materials and Processes in Manufacturing , Prentice-Hall, Englewood Cliffs, NJ, 1999.
- [Koelsch *et al.*, 1995] J.R. Koelsch, Thread milling takes on tapping, Manufacturing Engineering 115 (1995) 77–83.
- [Halas *et al* 1996]. D. Halas, Tapping vs. thread milling, Tooling and Production 62(1996) 99–102.
- [Dogra *et al.*, 2002] A.P.S. Dogra, S.G. Kapoor, R.E. DeVor, Mechanistic model for tapping process with emphasis on process faults and hole geometry , Journal of Manufacturing Science and Engineering 124 (2002)18–25.
- [Armarego *et al* 2002] E.J.A. Armarego, M.N.P. Chen, Predictive cutting models for the forces and torque in machine tapping with straight flutetaps, Cirp Annals—Manufacturing Technology 51 (2002) 75–78.
- [Campomanes *et al.*, 2002] M.L. Campomanes , Kinematics and dynamics of milling with roughing end mills, in: Metal Cutting and High Speed Machining ,Kluwer Academic Publishers, Plenum Press, Dordrecht, New York,2002.
- [Merdol *et al* 2004] S. Merdol, Y. Altintas, Mechanics and dynamics of serrated cylindrical and tapered end mills, Journal of Manufacturing Science and Engineering, Transactions of the ASME 126 (2) (2004) 317–326.
- [A.C. Araujo *et al.*, 2005] A.C. Araujo, J.L. Silveira, S.G. Kapoor, Force prediction in thread milling, Journal of the machine tool & manufacture (2005) 2057–2065
- [Budak *et al.*, 1996] Budak, E., Altintas, Y., Armarego, E.J.A., Prediction of Milling Force Coefficient from Orthogonal Cutting Data, 1st ed., Cambridge University Press, NY, USA, 1996.